Plasma Chemistry and Plasma Processing
https://doi.org/10.1007/s11090-021-10215-1

ORIGINAL PAPER

Effects of Dielectric Barrier Discharge Plasma on Physicochemical Characteristics, Mechanical Properties and Biocompatibility of Silk/PVA Nanofibers

Namita Ojah[1] · Susmita Thakur[2] · Dolly Gogoi[3] · Gazi Ameen Ahmed[1] · Manabendra Mandal[2] · Robin Doley[2] · Arup Jyoti Choudhury[1,4]

Received: 13 January 2021 / Accepted: 21 October 2021

Abstract
This work reports an investigation of the discharge characteristics of atmospheric dielectric barrier discharge (DBD) plasma in terms of I-V curves and Lissajous figures and their effect on the surface functionalities of electrospun silk/PVA nanofibers. The results show that the filamentary discharge is predominant at lower electrode gap (3 mm) and then significantly reduces at higher electrode gaps of 6 mm and 10 mm, respectively and in the applied voltage range of 11–17 kV. The silk/PVA nanofibers which are treated with 6 mm electrode gap shows good wettability, higher surface energy, higher tensile strength, young's modulus values and improved anti-thrombogenic property. All these findings suggest that, although the silk/PVA nanofiber itself can be used in biomedical applications however, nanofibers plasma treated at 6 mm electrode gap shows better results in terms of physical and biological performances.

Keywords Dielectric barrier discharges (DBD) · Plasma treatment · Surface modification · Mechanical properties, cell viability

Introduction

Silk fibroin based nanofibers have rapidly emerged as potential biomaterials for various biomedical applications [1–3]. The advantages of silk fibroin based nanofibers include but not limited to their outstanding properties such as biocompatilibity, flexibility, controlled microporous structure, large surface to volume ratio and morphology similar to that of native

✉ Arup Jyoti Choudhury
arupjchoudhury@gmail.com

[1] Laboratory for Plasma Processing of Materials, Department of Physics, Tezpur University, Napaam, Tezpur, Assam 784028, India

[2] Department of Molecular Biology and Biotechnology, Tezpur University, Napaam, Tezpur, Assam 784028, India

[3] Central Instruments Facility, Indian Institute of Technology, Guwahati, Assam 781039, India

[4] Department of Physics, Guwahati College, Bamunimaidam, Guwahati, Assam 781021, India

extracellular matrix [1–5]. Accordingly the silk fibroin based nanofibers have been widely explored as scaffolds for tissue engineering and wound dressing materials [4–6]. However, due to inherent hydrophobicity of silk fibroin and poor mechanical behavior of the nanofibers, preparation of silk fibroin based nanofibers and manipulation of their surface properties of still remains a challenge to fully explore their potential usage as biomaterials [7–10].

As a promising and versatile modification method, non-thermal plasma treatment has been extensively utilized in surface modification and functionalization of polymeric biomedical [11–14]. Due to its efficacy in controlling and reproducing the surface properties of polymers without affecting their bulk properties, versatility and environment friendly, selective treatment and sterilization of polymer surface in single step and improving surface biocompatibility for cell growth and proliferation and immobilization of bioactive proteins, non-thermal plasma treatment has drawn significant research interest in clinical applications and biomedical engineering [15–17]. Non-thermal plasma treatment further enables rapid processing of polymers with shorter treatment time without the use of any solvent and chemical as compared to wet surface modification [18–20].

Non-thermal plasma treatment has been used extensively to improve bioactivities of silk and silk-based biopolymers by modifying surface chemical composition and grafting specific functional groups onto the surface [16, 18, 20, 21]. Significant efforts have been made to investigate the effect of low pressure non-thermal plasma to enhance biocompatiblity and cellular interactions of silk and silk-based biopolymers whereas atmospheric pressure plasma is being less explored in this regard [16, 18, 20, 22]. Atmospheric pressure plasma has the advantage of processing and maintenance cost reduction and ease of operation without any need of sophisticated and expensive vacuum systems and therefore this technique can be utilized as an alternative to low pressure plasmas for surface modification of silk and silk-based biopolymers [15, 16]. In atmospheric pressure plasma, the efficiency of the plasma treatment is influenced by the processing parameters such as electrode gap, operating voltage, gas flow rate etc. and proper control of these parameters enables to sustain uniform glow discharges at atmospheric pressure which is important for effective and uniform surface treatment of silk and silk-based biopolymers [17, 19, 22–24]. Using optimized atmospheric pressure plasma treatment conditions, the potentialities of silk and silk-based biopolymers with improved hydrophilicity, mechanical robustness and biocompatibility can be explored in various biomedical and bioengineering applications [17–19, 22–24].

In this work, surface modification of silk/PVA nanofibers has been carried out using DBD plasma at atmospheric pressure. The operating plasma parameters are optimized to achieve uniform discharge for effective surface treatment of silk/PVA nanofibers. The effect of plasma treatment, at optimized discharge conditions, on physicochemical and mechanical properties and biocompatibility of silk/PVA nanofibers is further investigated. The untreated and plasma treated silk/PVA nanofibers are subjected to various characterization techniques and the observed properties are attempted to correlate with the optimized plasma discharge conditions.

Experimental

Materials

B. mori silk cocoons are collected from central silk board, Guwahati, Assam, India. Polyvinyl alcohol (PVA) of molecular weight 145 kDa is purchased from Merck, India. Sodium bicarbonate ($NaHCO_3 > 99\%$) and Lithium bromide ($LiBr > 99\%$) are supplied by Sigma

Aldrich, USA and Tokyo Chemical Industries, Japan, respectively. All chemical reagents are analytical reagent grade and used as received. The cellulose dialysis membrane (12 kDa molecular weight cut off) is supplied by Himedia, India.

Preparation of Silk Fibroin/PVA Solutions

B. mori silk fibroin solution is prepared as per the protocol previously described [16]. Briefly the raw *B. mori* silk cocoons are cut into pieces and boiled for 30 min in aqueous 0.02 M Na_2CO_3 and then rinsed thoroughly with water to extract the glue-like sericin proteins by means of the process known as degumming. The degummed silk is then dissolved in 9.3 M LiBr solution at 60 °C for 4 h yielding a 7% (w/v) solution. The dissolved solution is dialyzed against deionized water using 12 kDa dialysis membrane for 3 days with frequent change in water to remove the LiBr. The resulting solution is then centrifuged at 5000 rpm for 10 min to remove aggregates and debris. The purified SF solution is stored at 4 °C for further use.

An 8% (w/v) PVA solution is prepared by dissolving PVA in distilled water at 80 °C with vigorous stirring for a period about 3 h [16]. After cooling to room temperature, the PVA solution is kept overnight to remove trapped air bubbles. Afterward, both silk and PVA solutions are mixed at a ratio of 2:1 (silk: PVA) with mild stirring for 15 min at room temperature [18]. The final blend solution is kept at 4 °C until further use.

Electrospinning of Silk/PVA Solution

The electrospinning of blend silk/PVA solution is performed at room temperature. The schematic diagram of the method of *B. mori* silk fibroin solution preparation and the electrospinning setup is shown in Fig. 1A. The silk/PVA mixed solution is loaded into a 5 ml syringe with a 22 gauge stainless steel needle having an inner diameter of 0.6 mm. The positive electrode of a high voltage power supply is connected to the needle using an alligator clip and the nanofibers are collected on a grounded aluminum foil which is used as the collector. The high voltage is set at 18 kV, tip-to-collector distance was fixed at 12 cm and flow rate of the solution is maintained at 0.5 ml/hr. Finally, the aluminum foil with the electrospun nanofibrous mat is dried in vacuum for 12 h.

DBD Plasma Treatment

The schematic diagram of the experimental DBD setup and measurement is shown in Fig. 1B. The discharge is generated between two square plane-parallel copper electrodes with an area of 250 mm × 250 mm and both of them are covered by quartz glass plate with a thickness of 3 mm and an area of 250 mm × 250 mm as dielectric barrier. The upper electrode is connected with a high voltage power supply (0–40 kV, 50 Hz) and the lower electrode is connected to ground. The samples are placed on the grounded electrode which can be moved mechanically to adjust the discharge gap. The O_2 (Assam Air Products, purity > 99.99%) gas is allowed to enter the discharge chamber and the gas flow rate (2 slpm) is controlled by a digital mass flow controller (Alicat Scintific, USA). In this work, surface treatment of silk/PVA nanofibers is carried out at different discharge gap (3 mm, 6 mm and 10 mm) and in the applied voltage range of 11–17 kV (rms). Figure 1A shows the typical images (Nikon DSLR, D5200) of as prepared and

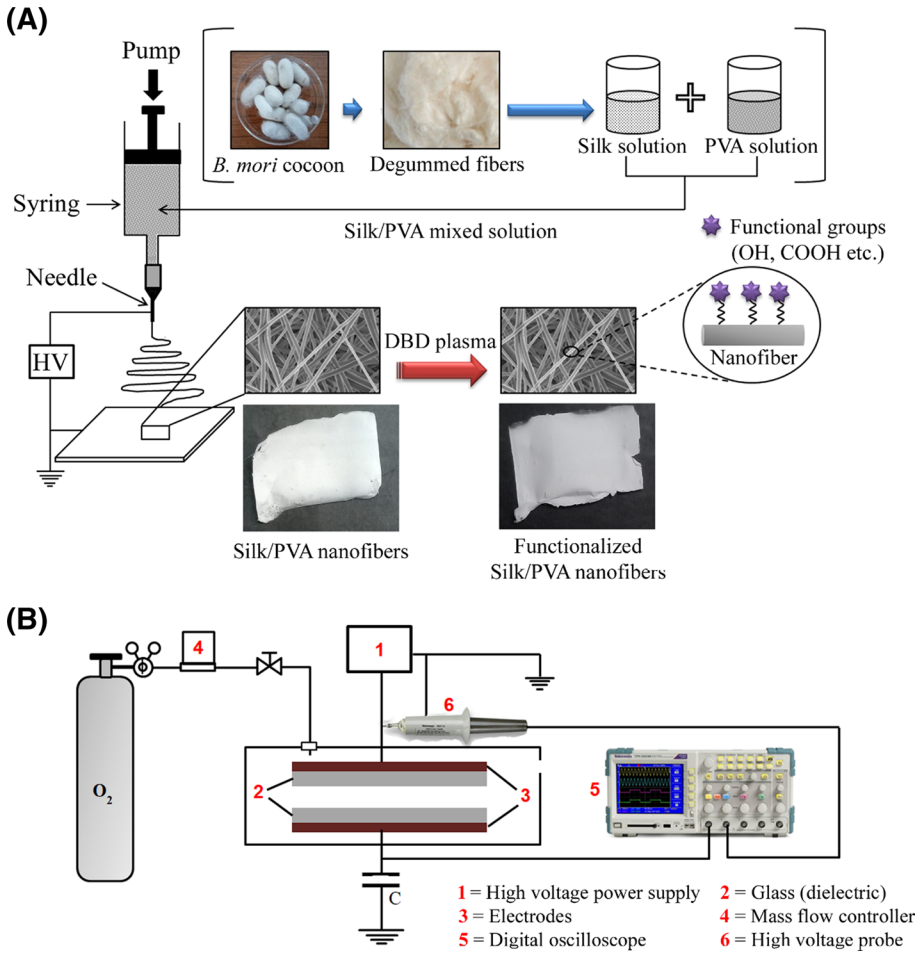

Fig. 1 **A** Schematic of the silk/PVA nanofibers preparation procedure. **B** Schematic diagram of the DBD plasma system and measurement set-up

plasma treated silk/PVA nanofibers obtained at discharge gap of 6 mm and applied voltage of 15 kV, where smooth and pinhole free surface with no morphological alteration due to plasma treatment can be observed.

The voltage applied to the upper electrode is measures using a high voltage probe (Tektronix P6015A, 1000:1) and the current–voltage waveforms are displayed in a dual channel digital oscilloscope (Tektronix TPS2024B, 200 MHz). The instantaneous charge, $Q(t)$ transported to the discharge is calculated by measuring the instantaneous voltage, $V_m(t)$ across capacitor (22 nF) that is connected in series to the ground electrode by applying the following relation [23],

$$Q(t) = C_m V_m(t) \tag{1}$$

where C_m is the capacitance of the capacitor.

A charge–voltage (Q–V) diagram, or Lissajous figure, is obtained by plotting instantaneous charge across the capacitor and the applied voltage against each other [23]. The energy which is consumed during one half-cycle of the discharge is then obtained by measuring the area of the Lissajous figure [23].

Characterization Techniques

Morphological characterization of untreated and plasma treated silk/PVA nanofibers is investigated by field emission electron microscope (FESEM) at 10 kV after sputter-coating with ultrathin layer of gold/palladium alloy. The average diameter of the nanofibers is determined by measuring around 150 nanofibers selected randomly from the FESEM images using Image J software.

The chemical compositions of silk/PVA nanofibers are analyzed by attenuated total reflectance Fourier transform infrared (ATR-FTIR) spectrometer (IMPACT 410 NICOLET, USA). The spectra are obtained as the mean of 32 scans taken in transmittance mode in the range of 650–4000 cm^{-1} with resolution of 4 cm^{-1} at room temperature.

To determine the wettability of silk/PVA nanofibers, the contact angle is measured by a contact angle measurement system (dataphysics OCA 20, Germany). The droplet size is set at 1 µL and immediately after dropping, the image is taken and stored via a CCD video camera, using a PC based acquisition and data processing system. To confirm the uniformity of electrospun nanofibers, the contact angle is measured 15 times at random points on the surface and the result is reported as mean ± standard deviation (SD). The surface energy is calculated by OWRK method using three different liquids (deionized water, n-hexane and diiodomethane).

The mechanical properties of the silk/PVA nanofibers are evaluated using a tensile tester (INSTRON 4204) at a constant speed of 5 mm min^{-1} with a 10 N load. Each sample is cut into rectangular strip with a length of 30 mm and a width of 10 mm. For each sample, data is taken for five times and the average of Young's modulus of elasticity, tensile strength and elongation at break (%) are evaluated from stress–strain curves. The results are presented as average ± standard deviation (SD) [15, 18].

Hemocompatibility Studies

Fresh Venous blood is collected from a healthy human donor in heparinized tubes, stored at 4 °C and used immediately after collection. The plasma treated (at discharge gaps of 6 mm and 10 mm, respectively and applied voltage range of 11–17 kV) and untreated silk/PVA nanofibers (0.5 cm^2) are incubated with 150 µL of human blood with 10% RBC suspension (prepared with 0.9% NaCl) and volume is adjusted to 2 ml with 0.9% NaCl followed by incubation for 1 h at 37 °C. Blood incubated with 0.9% NaCl is considers as negative control as well as with distilled water without test material is considered as positive control for the test. After 1 h of incubation, the reaction mixture is centrifuged at 10,000 rpm for 10 min and the supernatant is carefully collected. The free hemoglobin present in the supernatant is measured using a UV–visible spectrophotometer at wavelength 540 nm. The percentage of hemolysis is calculated using the following relation,

$$\text{Hemolysis (\%)} = \frac{Abs_{sample} - Abs_{-vecontrol}}{Abs_{+vecontrol} - Abs_{-vecontrol}} \times 100 \quad (2)$$

MTT Assay Test

The cell viability after growth on the silk/PVA nanofibers (untreated and plasma treated) are evaluated by the MTT (3-[4,5-dimethylthiazole- 2-yl]-2,5-diphenyltetrazolium bromide) assay in human embryonoc kidney (HEK293T) cells. Briefly, HEK293T cells are plated in 96 well plates and exposed with 1 mg/ml concentration of different samples for 24 h. MTT is added to each well and incubated for 4 h at 37 °C. On termination of incubations, formazan crystals formed in cells are dissolved in acidic isopropanol and incubated further for 30 min at 37 °C. Cytotoxicity is measured spectrophotometrically at 570 nm with Varioskan LUX Multimode Microplate Reader (Thermo Scientific, Finland). Absorbance values are blanked against acidic isopropanol and the absorbance of cells exposed to medium only (without any treatment) are taken as 100% cell viability (control). The percentage of cell viability is calculated by using the following formula.

$$\text{Cell viability (\%)} = \frac{N_t}{N_c} \times 100 \quad (3)$$

where N_t and N_c are absorbance of the treated and untreated cells. All experiments are performed in triplicate and data are expressed as mean ± standard deviation (SD).

In-Vitro Antithrombogenic Property

The antithrombogenic properties of these silk/PVA nanofibers are evaluated using an in-vitro kinetic method. 1 ml of anticoagulant citrate dextrose (ACD) blood is incubated in micro centrifuge tubes each containing the silk/PVA nanofibers (untreated and plasma treated) separately at 37 °C without shaking. After 1 h of incubation, 0.2 ml of blood is taken out from each tube and placed on a clean sterilized glass plate. Prior to the experiment, the glass plates are sterilized by autoclaving at high pressure saturated steam at 121 °C for 30 min. The clotting is initiated by addition of 0.02 ml 0.1 M $CaCl_2$ to the citrated blood. After 15 min and 60 min intervals respectively, the blood clot formed on each glass plate is scrapped and fixed in 2 ml formaldehyde solution (36% v/v) for 10 min, then washed with distilled water, blotted with tissue paper and weighed. The ACD blood alone, without any sample incubation, is considered as control. The experiment is carried out in triplicates and the results are reported as mean ± standard deviation (SD).

Statistical Analysis

All the data were statistically analyzed and expressed as the mean ± standard deviation (SD). The significance of the differences among the tested samples are determined by one-way analysis of variance (ANOVA) followed by Tukey test for multiple comparisons (Origin Lab OriginV8.6 Software). P values < 0.05 is considered statistically significant for hemocompatibility and MTT assay studies. $P < 0.008$ is considered statistically significant for water contact angle measurements.

Results and Discussions

Electrical Characterization of DBD Plasma

The respective voltage and current waveform for the DBD plasma at three different electrode gaps (3 mm, 6 mm and 10 mm) and applied voltage range of 11–17 kV with an interval of 2 kV is shown in Fig. 2A–L. As seen from Fig. 2A–D, filamentary discharge is observed at electrode gap of 3 mm, characterized by the spikes that appear in the current waveform and is found to sustain in the entire voltage range of 11–17 kV. For electrode gaps of 6 mm and 10 mm (Fig. 2E–L), filamentary discharge is significantly reduced at all applied voltages (11–17 kV) as revealed by single current pulse per half-cycle of the applied voltage with the same periodicity. Furthermore, from visual observation it is seen that by increasing the electrode gap above 3 mm, the filaments diminish and the discharge uniformly spreads over the entire surface of the electrode. This possibly results in uniform surface treatment of silk/PVA nanofibers without any structural damage which is evident from Fig. 1A where smooth surface, free of pinholes, can be observed. As uniform surface treatment of polymer is more preferred for desirable properties, the characterization results of silk/PVA nanofibers treated at electrode gaps of 6 mm and 10 mm, respectively and applied voltage range of 11–17 kV are considered for further discussions in this work.

Figure 3A–C show the Lissajous figures of the DBD discharge at different electrode gaps and applied voltages. From the area of the respective Lissajous figure, the energy dissipated during one half-cycle of the discharge is calculated and the results are presented in Fig. 3D. It is evident that lowering in energy dissipation in the discharge is associated with decrease in electric field strength with increase in electrode discharge gap for a particular applied voltage. Although higher energy dissipation takes place at electrode gap of 3 mm and applied voltage range of 11–17 kV, the occurrence of high degree of filamentary discharge under these experimental conditions does not seemed to be appropriate for uniform surface treatment of silk/PVA nanofibers.

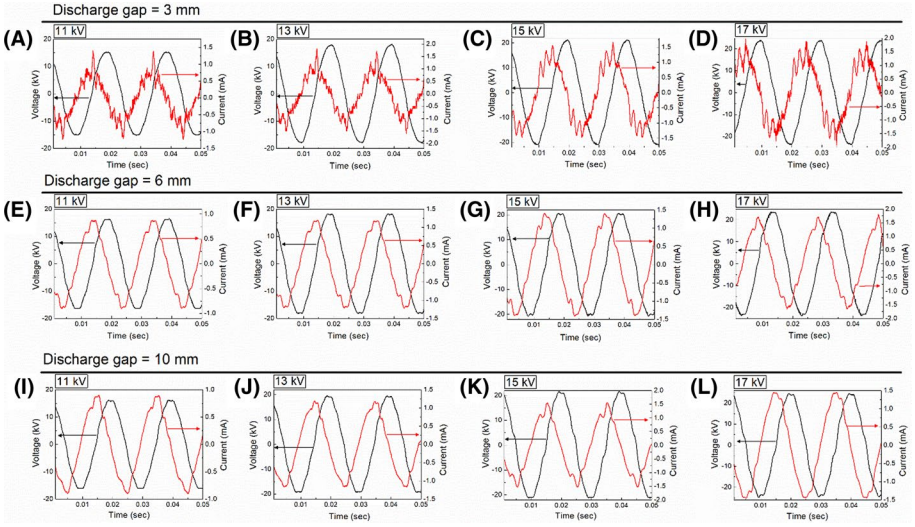

Fig. 2 **A–L** Voltage and current waveforms with different discharge gaps and applied voltages

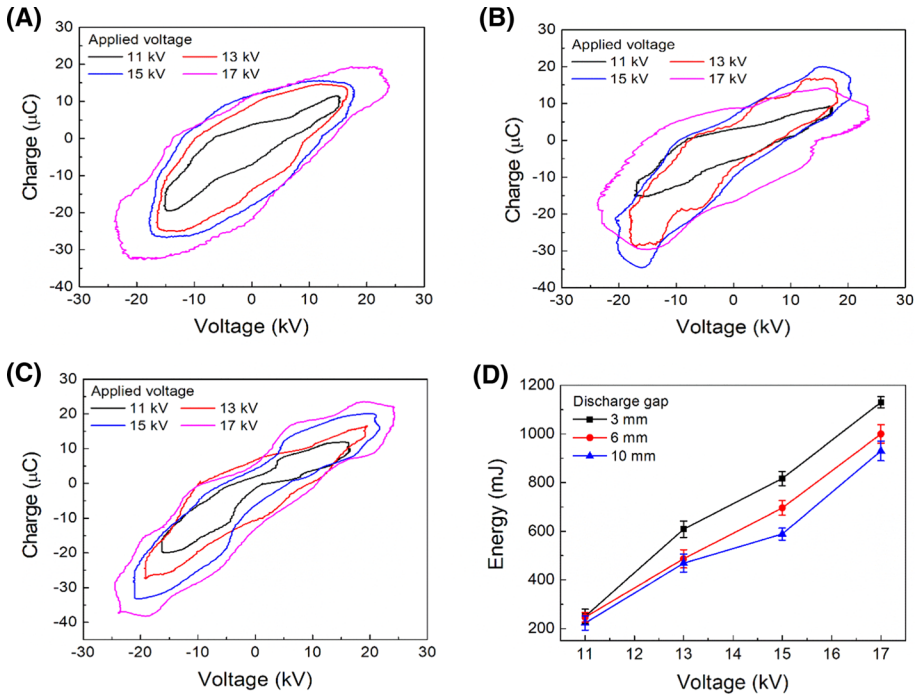

Fig. 3 Lissajous figures for discharge gaps at **A** 3 mm, **B** 6 mm and **C** 10 mm, respectively. **D** Variation of electric energy dissipation in the DBD discharge with applied voltage

From these experimental observations, it may be suggested that above discharge gap of 3 mm and in the voltage range of 11–17 kV, the discharge becomes more macroscopically homogeneous although complete elimination of filamentary discharge under the present investigation cannot be confirmed.

Surface Morphology of Silk/PVA Nanofibers

The FESEM images show morphology of untreated and plasma treated silk/PVA nanofibers with wide and uneven nanofiber diameter distribution (Fig. 4A–I). The nanofibers are obtained with smooth fiber morphology without the presence of beads. The average diameter of untreated silk/PVA nanofibers is evaluated to be 150 ± 23 nm. It is observed that DBD plasma treatment does not significantly alter the surface structure and morphology of silk/PVA nanofibers as the average fiber diameter, after plasma treatment, is found to be in the range of 149–153 nm. FESEM analyses clearly shows that in this present work, DBD plasma treatment applied under various discharge conditions causes no structural and morphological damage to the silk/PVA nanofibers and the DBD plasma can be utilized as an effective and non-destructive method for treating silk and silk-based polymeric surfaces [16–18].

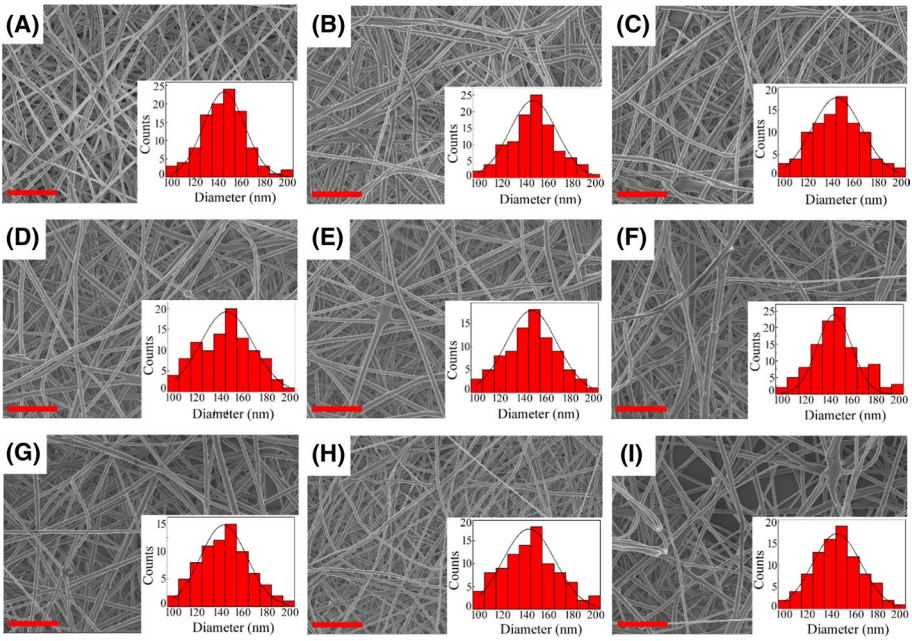

Fig. 4 FESEM images of **A** untreated silk/PVA nanofibers; plasma treated nanofibers at discharge gap of 6 mm and applied voltages of **B** 11 kV, **C** 13 kV, **D** 15 kV and **E** 17 kV, respectively and plasma treated nanofibers at discharge gap of 10 mm and applied voltages of **F** 11 kV, **G** 13 kV, **H** 15 kV and **I** 17 kV, respectively. The insets show the diameter distribution of untreated and plasma treated silk/PVA nanofibers, respectively. AMOX-BMSF/PVA and AMOX-BMSF/PVA/O_2 nanofibers, respectively (FESEM image, scale: 1 µm)

Water Contact Angle Measurement

In this work, the wettability of silk/PVA nanofibers, before and after plasma treatment is studied using water contact angle measurements and the results are presented in Table 1. It is evident that the plasma treatment results in lowering in water contact angle and subsequent increase in surface energy of silk/PVA nanofibers, which is attributed to surface functionalization of the nanofibers with oxygen containing functional groups such as –OH, –C = O, –O–C–O, COOH etc., [16, 18, 20]. An increase in the content of polar components onto the surface of silk/PVA nanofibers also corroborates the inference. It is further observed that surface hydrophilicity is more pronounced for silk/PVA nanofibers treated at discharge gap of 6 mm as compared to that of 10 mm discharge gap. Moreover, surface hydrophilicity of silk/PVA nanofibers is observed to be increased with applied voltage. These results are strongly related to the dissipation of more energy in the plasma at smaller discharge gap as well as increase of applied voltage at a particular discharge gap. This leads to high degree of dissociation and ionization of gas molecules and formation of reactive plasma species such as free radicals, excited metastable atoms/molecules and ions and subsequently facilitates more heterogeneous reactions between the surface of the nanofibers exposed to the plasma and the plasma species.

Table 1 Contact angle and surface free energy of untreated and plasma treated silk/PVA nanofibers at different discharge parameters (mean ± standard deviation (SD))

Plasma treatment conditions		Water contact angle (°)	Polar component (mJm^{-2})	Dispersive component (mJm^{-2})	Total surface energy (mJm^{-2})
Untreated silk/PVA nanofibers		77.1 ± 1.7	4.8 ± 0.5	40.3 ± 1.4	45.1 ± 1.1
Plasma treated silk/PVA nanofibers					
Applied voltage (kV)	Electrode gap (mm)				
11	6	36.8 ± 1.2	27.4 ± 1.5	37.2 ± 1.2	64.6 ± 3.1
13		33.2 ± 1.1	26.4 ± 1.4	39.5 ± 1.8	65.9 ± 2.4
15		21.6 ± 1.6	33.4 ± 1.8	39.2 ± 1.7	72.6 ± 2.9
17		22.2 ± 1.5	34.5 ± 1.1	37.5 ± 1.4	72.0 ± 2.4
11	10	58.3 ± 1.8	12.1 ± 1.2	44.3 ± 2.1	56.4 ± 1.9
13		47.5 ± 1.4	17.2 ± 1.4	42.0 ± 2.5	59.2 ± 1.5
15		43.5 ± 2.0	25.1 ± 1.0	37.2 ± 1.7	62.3 ± 1.7
17		42.6 ± 1.6	24.4 ± 1.9	38.1 ± 1.5	62.5 ± 1.8

ATR-IR Spectra Analyses

Figure 5A shows the ATR-IR spectra of PVA, BMSF and silk/PVA nanofibers. In the spectrum of PVA, a broad band appears in the region, 3100–3650 cm^{-1}, which is assigned as the absorption due to the OH stretching vibration from intermolecular and intramolecular hydrogen bonds of PVA [16]. The peaks at 2940 cm^{-1} and 2907 cm^{-1} are assigned to the symmetric and asymmetric CH stretching vibrations of alkyl groups, respectively [16, 25]. The characteristics of carbonyl group of PVA are found at 1645 cm^{-1} and 1533 cm^{-1} which are attributed to the C–O stretching vibrations and C = C stretching vibrations, respectively [16, 25]. The peaks that are observed at 1410 cm^{-1}, 1323 cm^{-1}, 1227 cm^{-1} and 1085 cm^{-1} correspond to the CH_2 bending, CH deformation, CH wagging and C-O stretching vibrations of acetyl group, respectively [16, 25]. The ATR-IR spectrum shows the characteristics peaks of BMSF at 1622 cm^{-1}, 1515 cm^{-1} and 1224 cm^{-1} which correspond to amide I, amide II and amide III groups, respectively [16, 18, 25]. The broad band appeared in

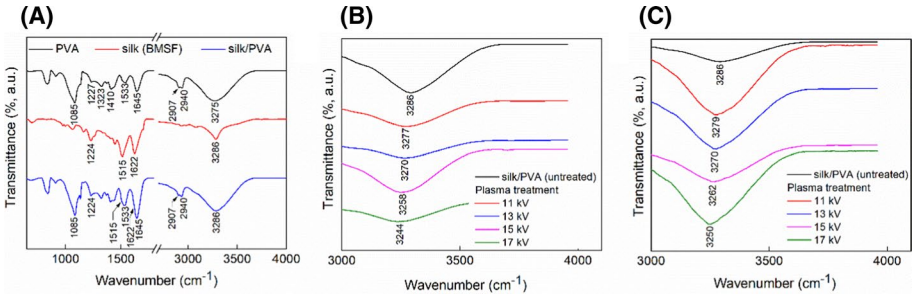

Fig. 5 ATR-IR spectra of **A** PVA, BMSF and silk/PVA nanofibers; untreated and plasma treated silk/PVA nanofibers at discharge gaps of **B** 6 mm and **C** 10 mm, respectively and applied voltage range of 11–17 kV

the region, 3100–3650 cm^{-1}, is due to the overlapping of the stretching vibrations of primary amino group (NH) and hydrogen bonded OH groups [16, 20, 24]. Moreover, in the ATR-IR spectra of composite nanofiber of silk/PVA both the peaks of PVA as well as silk has appeared. The presence of the absorption bands/peaks of PVA and BMSF in the ATR-FTIR spectrum of silk/PVA nanofibers confirms the successful formation of the composite nanofibers.

The ATR-IR spectra of plasma treated silk/PVA nanofibers at discharge gaps of 6 mm and 10 mm, respectively and applied voltage range of 11–17 kV are plotted in the region of interest (3000–4000 cm^{-1}) and shown in Fig. 5B, C. The plasma treatment does not seem to induce any change in the characteristic peaks of PVA and BMSF in the lower wavenumber region (650–3000 cm^{-1}). However, the band positioned in the region 3100–3650 cm^{-1} is found to be shifted towards lower wavenumber with increase in applied voltage (11–17 kV) and at different electrode gaps, which indicates incorporation of polar functional groups (e.g. hydroxyl, carboxyl, carboxylate etc.) through formation of hydrogen bonds on to the surface of silk/PVA nanofibers [18]. The hydrogen bond formation is facilitated mainly by the different highly reactive plasma species that are generated during air/O_2 plasma treatment and their subsequent interaction with the surface of silk/PVA nanofibers [16]. These polar groups are responsible for enhancing surface free energy and wettability of silk/PVA nanofibers which is well evident from earlier discussions on contact angle measurement.

Mechanical Analysis

The tensile strength, Young's modulus and elongation at break (%) of silk/PVA nanofibers are investigated before and after plasma treatment and the results are presented in Table 2. It is observed that tensile strength and Young's modulus of plasma treated silk/PVA nanofibers are higher than the untreated nanofibers, which is contributed by the interaction of polar groups with the surface of silk/PVA nanofibers through formation of hydrogen bonds which subsequently results in efficient load transfer in the nanofibers [18, 20]. However, decrease in elongation at break indicates relatively higher degree of stiffness in

Table 2 Mechanical properties of untreated and plasma treated silk/PVA nanofibers at different discharge parameters (mean ± standard deviation (SD))

Mechanical properties	silk/PVA (untreated)	Applied voltage (kV)	Electrode gap	
			6 mm	10 mm
Tensile strength (MPa)	5.25 ± 0.33	11	5.40 ± 0.43	5.31 ± 0.52
		13	5.47 ± 0.51	5.40 ± 0.40
		15	6.11 ± 0.60	5.80 ± 0.62
		17	6.44 ± 0.55	6.02 ± 0.53
Young's modulus (MPa)	37.60 ± 2.25	11	39.23 ± 2.54	38.12 ± 2.44
		13	40.11 ± 2.61	38.50 ± 2.52
		15	44.52 ± 2.70	40.53 ± 2.80
		17	47.34 ± 2.81	42.44 ± 2.83
Elongation at break (%)	38.01 ± 2.01	11	35.20 ± 1.54	37.40 ± 1.64
		13	35.05 ± 2.05	36.00 ± 2.84
		15	33.02 ± 2.01	34.85 ± 1.67
		17	30.10 ± 1.74	31.15 ± 1.87

plasma treated silk/PVA nanofibers compared to the untreated nanofibers [16, 18]. It is further observed that the increase in tensile strength and Young's modulus in plasma treated silk/PVA nanofibers is more prominent at and above applied voltage of 15 kV which suggest that plasma treatment up to the applied voltage of 13 kV may not be effective in modifying the surface properties of silk/PVA nanofibers. For silk/PVA nanofibers treated at discharge gap of 6 mm, the percentage increase in tensile strength and Young's modulus is observed to be 4.20% and 6.70% respectively. However, the tensile strength and Young's modulus increases to 16.40% and 18.42%, respectively at applied voltage of 15 kV and it reaches up to 22.70% and 26.00%, respectively with increase in applied voltage to 17 kV. Similar inference can be drawn for silk/PVA nanofibers treated at discharge gap of 10 mm and applied voltage range of 11–17 kV. Furthermore, silk/PVA nanofibers treated at discharge gap of 6 mm shows higher values of tensile strength and Young's modulus as compared to that treated at discharge gap of 10 mm. This is accounted for dissipation of higher electrical energy at discharge gap of 6 mm which eventually leads to high degree of hydrogen bonding interaction between the polar groups and the surface of silk/PVA nanofibers.

Hemocompatibility and Cell Viability Assays

Hemoysis study provides a useful tool for assessing blood compatibility of materials and can hold significant implications for biomedical use. As per the ASTM standards (F756-17), materials exhibiting percentage of hemolysis less than 2% is considered as non-hemolytic and suitable for use in biomedical application [18]. The hemolysis studies of untreated and plasma treated silk/PVA nanofibers are performed for the evaluation of hemocompatibility and the results are shown in Fig. 6A. The results show that the percentage of hemolysis for all the test samples is far below the permissible limit and thus indicate that no cytotoxic effects are caused by silk/PVA nanofibers and plasma treatment, regardless of change in applied voltage and discharge gap, does not affect the hemolytic activity of the nanofibers.

The results of in vitro cytotoxicity studies of the untreated and plasma treated silk/PVA nanofibers at various discharge parameters are shown in Fig. 6B, C. The cell viability of the untreated silk/PVA nanofibers is observed to be increased with higher incubation period which clearly indicates that the nanofibers do not have any toxic effect on the HEK293T cells, but rather increases the viability of cells. For silk/PVA nanofibers treated at discharge gap of 6 mm, noticeable increase in cell viability is observed at applied

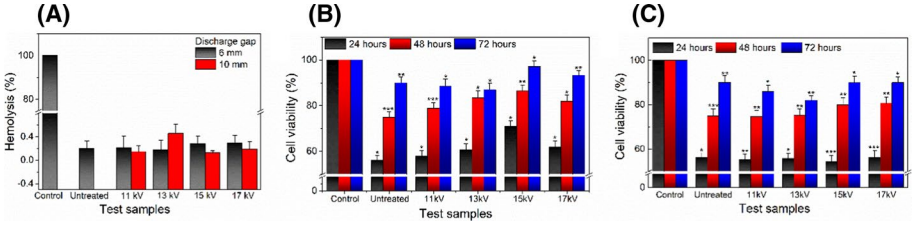

Fig. 6 **A** Hemocompatibility studies of the untreated and plasma treated silk/PVA nanofibers at discharge gaps of 6 mm and 10 mm, respectively and applied voltage range of 11–17 kV. Viability (%) of human embryonoc kidney (HEK293T) cells at different post incubation periods with untreated and plasma treated silk/PVA nanofibers at discharge gaps of **B** 6 mm and **C** 10 mm, respectively. (***, ** and * show significant differences from control at $p < 0.01$, $p < 0.02$ and $p < 0.05$, respectively). Values represent mean ± SD of three batches. Control: cell with no treatment

voltage of 15 kV, after incubation period of 24 h, as compared to the untreated one. After incubation period of 48 h, the cell viability of silk/PVA nanofibers moderately increases up to applied voltage of 15 kV while no significant change in cellular viability is observed in the nanofibers treated in the applied voltage range of 11–13 kV, as observed after 72 h of incubation period. During the entire incubation period, silk/PVA nanofibers treated at applied voltage of 15 kV displays better activity with regard to cell proliferation capability among the untreated and other plasma treated nanofibers. At applied voltage of 17 kV, a minor decrease in cellular viability is observed for silk/PVA nanofibers, although it still remains higher as compared to those treated at lower applied voltages (11–13 kV). The improvement in cell viability of silk/PVA nanofibers treated at applied voltage of 15 kV and 17 kV and after incubation period of 72 h is attributed to the enhanced hydrophilicity due to incorporation of more polar functional groups onto the surface.

At discharge gap of 10 mm and after incubation period of 24 h, cell viability of plasma treated silk/PVA nanofibers is similar to the untreated one and with increase in applied voltage (11–17 kV) no changes can be observed in cell viability of the nanofibers. After incubation period of 48 h, similar observations can be made for silk/PVA nanofibers treated at applied voltages of 11 kV and 13 kV although those treated at and above applied voltage of 15 kV shows improvement in cellular viability. At higher applied voltage of 15 kV and 17 kV, respectively, the silk/PVA nanofibers displays cell viability similar to the untreated one, as observed after incubation period of 72 h. The results suggest that at discharge gap of 10 mm and in the applied voltage range of 11–17 kV, the energy dissipated in the plasma may not be effective in altering the surface properties of silk/PVA nanofibers. The overall observations indicate that plasma treated silk/PVA nanofibers do not show any adverse effect on cell proliferation and viability and that these biomaterials can be considered suitable for tissue engineering [18].

In vitro Antithrombogenic Activity

The antithrombogenic activity of the untreated and plasma treated silk/PVA nanofibers are further evaluated in this work and the results are presented in Table 3. It is evident that weight of thrombus formation increases with increase in blood coagulation time. As observed from the data presented in Table 3, the untreated silk/PVA nanofibers alone do not show significant effect on antithrombogenic activity which suggests that the nanofibers are compatible with human erythrocytes. At discharge gap of 6 mm, the silk/PVA nanofibers treated at applied voltage of 11 kV and 13 kV respectively shows no change in antithrombogenic activity in comparison with the control. However, with further increase in applied voltage at and above 15 kV, silk/PVA nanofibers begin to show reduction in the weight of thrombus formation. The improvement in antithrombogenicity of plasma treated silk/PVA nanofibers at applied voltage of 15 kV and may be associated with their enhanced surface free energies due to incorporation of polar functional groups onto the surface.

At discharge gap of 10 mm and applied voltage range of 11–13 kV, the silk/PVA nanofibers show antithrombogenic activity similar to that of the control although an improvement in the observed property can be seen at and above applied voltage of 15 kV. At observation period of 60 min, no significant changes in antithrombogenicity of the silk/PVA nanofibers, treated at applied voltage range of 11–17 kV, can be observed which suggests that at these particular discharge conditions, the DBD plasma treatment may not be effective in improving the blood compatibility of the nanofibers.

Table 3 Measurement of thrombus (mg) formed after 15 and 60 min of observation period for untreated and plasma treated silk/PVA nanofibers at different discharge parameters (mean ± standard deviation (SD))

	Sample	Observation time (Minutes)	
		15	60
		Weight of thrombosis (mg)	
	Control	57.15 ± 2.33	110.75 ± 2.84
	Silk/PVA nanofibers (Untreated)	55.04 ± 2.14	108.35 ± 2.54
Electrode gap (mm)	Applied voltage (kV)		
6	11	56.25 ± 2.35	104.50 ± 2.53
	13	52.75 ± 2.33	102.20 ± 2.70
	15	31.04 ± 1.65	75.15 ± 2.75
	17	32.30 ± 1.70	74.70 ± 2.13
10	11	56.22 ± 2.61	105.54 ± 2.41
	13	57.51 ± 3.14	104.62 ± 3.25
	15	47.00 ± 1.82	106.60 ± 2.74
	17	44.25 ± 1.75	105.25 ± 3.17

Conclusions

The present study investigates the effect of atmospheric DBD plasma modification on surface properties and biocompatibility of silk/PVA nanofibers. For uniform surface modification of the nanofibers, the electrical characteristics of DBD plasma are investigated at different electrode gaps and applied voltages. At discharge gaps of 6 mm and 10 mm and applied voltage range of 11–17 kV, uniform and lower degree of filamentary glow discharge is observed and subsequently surface treatment of the silk/PVA nanofibers is carried out under these discharge conditions. It is observed that the silk/PVA nanofibers treated at discharge gap of 6 mm and applied voltage range of 11–17 kV shows high degree of surface wettability and mechanical strength as compared to the untreated one and those treated at discharge gap of 10 mm. It is apparent that dissipation of more energy in the plasma at smaller discharge gap which results in incorporation of more polar groups onto the surface and an increase in hydrogen bonding interaction between the polar groups and the surface of the silk/PVA nanofibers is mainly responsible for improvement in the observed properties of the nanofibers. The hemolysis and antithrombogenic studies reveal that DBD plasma treatment does not seemed to compromise but improve the blood compatibility of silk/PVA nanofibers. Furthermore, the silk/PVA nanofibers treated at optimized applied voltage of 15 kV and discharge gap of 6 mm, exhibit better ability of cell adhesion and proliferation onto the surface as compared to the untreated nanofibers. The results reported in this work clearly suggest that the DBD plasma treated silk/PVA nanofibers can be explored as wound dressing in clinical applications.

Acknowledgements This research work is supported by DST-SERB (Grant No. SR/FTP/ PS-147/2012 and EMR/2016/006146) funded by Department of Science and Technology (DST), India. Arup Jyoti Choudhury expresses his gratitude to the DST-INSPIRE Faculty Fellowship (Grant No. IFA14-PH-93) for the financial support to carry out this research work and the Tezpur University, Assam, India for hosting the fellowship. Namita Ojah acknowledges the support provided by DST (India) in the form of fellowship under DST-INSPIRE Faculty program. The assistance of Mr. Kaushik Nath and Dr. Suman Dasgupta from Department

of Physics and Department of Molecular Biology and Biotechnology, Tezpur University, 784028, Assam, India in carrying out the antithrombogenic test and MTT cell viability study is sincerely acknowledged.

References

1. Zhang X, Tsukada M, Morikawa H, Aojima K, Zhang G, Miura M (2011) Production of silk sericin/silk fibroin blend nanofibers. Nanosc Res lett 6:510
2. Jeong L, Yeo IS, Kim HN, Yoon YI, Jang DH, Jung SY, Min BM, Park WH (2012) In vivo evaluation of porous hydroxyapatite/chitosan-alginate composite scaffolds for bone tissue engineering. Int J Biol Macrom 51:1079
3. Shao W, He J, Sang F, Ding B, Chen L, Cui S, Kejing L, Han Q, Tan W (2016) Coaxial electrospun aligned tussah silk fibroin nanostructured fiber scaffolds embedded with hydroxyapatite–tussah silk fibroin nanoparticles for bone tissue engineering. Mater Sci Engg C 58:342
4. Min K, Kim S, Kim S (2018) Silk protein nanofibers for highly efficient, eco-friendly, optically translucent, and multifunctional air filters. Sci Reports 8:9598
5. Yang W, Li R, Fang C, Hao W (2019) Surface modification of polyamide nanofiber membranes by polyurethane to simultaneously improve their mechanical strength and hydrophobicity for breathable and waterproof applications. Prog Org Coat 131:67
6. Kim HJ, Park SJ, Park CS, Le TH, Lee SH, Ha TH, Kim HI, Kim J, Lee CS, Yoon H, Kwon OS (2018) Surface-modified polymer nanofiber membrane for high-efficiency microdust capturing. Chem Engg J 339:204
7. Jin HJ, Fridrikh SV, Rutledge GC, Kaplan DL (2002) Electrospinning Bombyx mori silk with poly (ethylene oxide). Biomacromol 3:1233
8. Yao J, Bastiaansen CWM, Peijs T (2014) High strength and high modulus electrospun nanofibers. Fibers 2:158
9. Nakashima R, Watanabe K, Lee Y, Kim BS, Kim IS (2013) Mechanical properties of poly (vinylidene fluoride) nanofiber filaments prepared by electrospinning and twisting. Adv Polym Tech 32:44
10. Chaivan P, Pasaja N, Boonyawan D, Suanpoot P, Vilaithong T (2005) Low-temperature plasma treatment for hydrophobicity improvement of silk. Sur Coat Tech 193:356
11. Kingshott P, Andersson G, McArthur SL, Griesser HJ (2011) Surface modification and chemical surface analysis of biomaterials. Curr Opinion Chem Bio 15:667
12. Bhurke AS, Askeland PA, Drzal LT (2007) Surface modification of polycarbonate by ultraviolet radiation and ozone. J Adhesion 83:43
13. Kim SE, Wang J, Jordan AM, Korley LTJ, Baer E, Pokorski JK (2014) Surface modification of melt extruded poly (ε-caprolactone) nanofibers: toward a new scalable biomaterial scaffold. ACS Macro Lett 3:585
14. Yoo HS, Kim TG, Park TG (2009) Surface-functionalized electrospun nanofibers for tissue engineering and drug delivery. Adv Drug Deliv Rev 61:1033
15. Das P, Ojah N, Kandimalla R, Mohan K, Gogoi D, Dolui SK, Choudhury AJ (2018) Surface modification of electrospun PVA/chitosan nanofibers by dielectric barrier discharge plasma at atmospheric pressure and studies of their mechanical properties and biocompatibility. Int J Bio Macromol 114:1026
16. Ojah N, Saikia D, Gogoi D, Baishya P, Ahmed GA, Ramteke A, Choudhury AJ (2019) Surface modification of core-shell silk/PVA nanofibers by oxygen dielectric barrier discharge plasma: studies of physico-chemical properties and drug release behavior. App Sur Sci 475:219
17. Rajasekaran P, Mertmann P, Bibinov N, Wandke D, Viol W, Awakowicz P (2010) Filamentary and homogeneous modes of dielectric barrier discharge (DBD) in air: investigation through plasma characterization and simulation of surface irradiation. Plasma Process Polym 7:665
18. Ojah N, Borah R, Ahmed GA, Mandal M, Choudhury AJ (2020) Surface modification of electrospun silk/AMOX/PVA nanofibers by dielectric barrier discharge plasma: physiochemical properties, drug delivery and in-vitro biocompatibility. Prog In Biomater 9:219
19. Miao C, Liu F, Wang Q, Cai M, Fang Z (2018) Investigation on the influence of electrode geometry on characteristics of coaxial dielectric barrier discharge reactor driven by an oscillating microsecond pulsed power supply. Eur Phys J D 72:57
20. Ojah N, Deka J, Haloi S, Kandimalla R, Gogoi D, Medhi T, Mandal M, Ahmed GA, Choudhury AJ (2019) Chitosan coated silk fibroin surface modified by atmospheric dielectric-barrier discharge (DBD) plasma: a mechanically robust drug release system. J Biomater Sci Polym Ed 30:1142
21. Zhu L, Xu W, Ma M, Zhou H (2010) Effect of plasma treatment of silk fibroin powder on the properties of silk fibroin powder/polyurethane blend film. Polym Eng Sci 50:1705

22. Long JJ, Wang HW, Lu TQ, Tang RC, Zhu YW (2008) Application of low-pressure plasma pretreatment in silk fabric degumming process. Plasma Chem Plasma Process 28:701
23. Wang C, Zhang G, Wang X (2012) Comparisons of discharge characteristics of a dielectric barrier discharge with different electrode structures. Vacuum 86:960
24. Choo K, Ching YC, Chuah CH, Julai S, Li NS (2016) Preparation and characterization of polyvinyl alcohol-chitosan composite films reinforced with cellulose nanofiber. Mater 9:644
25. Zhou J, Cao C, Ma X (2009) A novel three-dimensional tubular scaffold prepared from silk fibroin by electrospinning. Int J Bio Macromol 45:504